Adaptive Modulation and Coding Simulations for Mobile Communication Networks

Nizar Zarka, Amoon Khalil and Abdelnasser Assimi
Higher Institute for Applied Sciences and Technology
Communication Department
Damascus, Syria
Email: nizar.zarka@hiast.edu.sy

Abstract—This paper presents the simulations of Adaptive Modulation and Coding (AMC) for Mobile Communication Networks. The simulations show that AMC gives higher throughput than the static modulation and coding with a gain of $4dB$ of the Signal-to-Noise Ratio (SNR). The simulation results are validated using real measurements of the High Speed Packet Access Evolution (HSPA+) mobile network.

I. INTRODUCTION

The increasing demand of mobile multimedia services including VoIP, mobile TV, audio and video streaming, video conferencing, FTP and internet access require intelligent communication systems able to adapt the transmission parameters based on the link quality. Changing the modulation and coding scheme yield a higher throughput by transmitting with high information rates under favorable channel conditions and reducing the information rate in response to degradation effects of the channel [1]. The idea behind the Adaptive Modulation and Coding (AMC) is to dynamically change the modulation and coding scheme to the channel conditions. If good Signal-to-Noise Ratio (SNR) is achieved, system can switch to the highest order modulation with highest code rates (e.g. $64-QAM$ with code rate $CR = \frac{3}{4}$). If channel condition changes, system can shift to other low order modulation with low code rates (e.g. $QPSK$ with $CR = \frac{1}{2}$) [3].

The aim of this paper is to understand how AMC works, to develop our own simulation tools and validate the simulation results with the real measurements of the HSPA+ mobile network [2]. The paper is organized as follows; first we present the design of the proposed system model for mobile communication networks, followed by the simulation results of the static and the adaptive modulation and coding and the validation from real measurements and finally a conclusion.

II. PROPOSED SYSTEM MODEL

Figure 1 represents the simulation model used in our simulation program. It is composed of a transmitter, a communication channel and a receiver. At the transmitter U_n data are encoded to get C_n using Turbo code with rate $\frac{1}{3}$. Some symbols are removed in the puncturing block to give D_n depending on the code rate $CR = \frac{1}{3}$, $CR = \frac{1}{2}$ or $CR = \frac{2}{3}$ [4]. The modulation

used are $QPSK$, $16-QAM$ or $64-QAM$. The modulated complex symbols are sent to an Additive White Gaussian Noise channel (AWGN). At the receiver a soft demodulation is applied to get LLR followed by a de-puncturing where zeros are added to the removed symbols during the puncturing phase. Finally symbols are detected in the Turbo decoder V_n. In the following we will describe each part of the system.
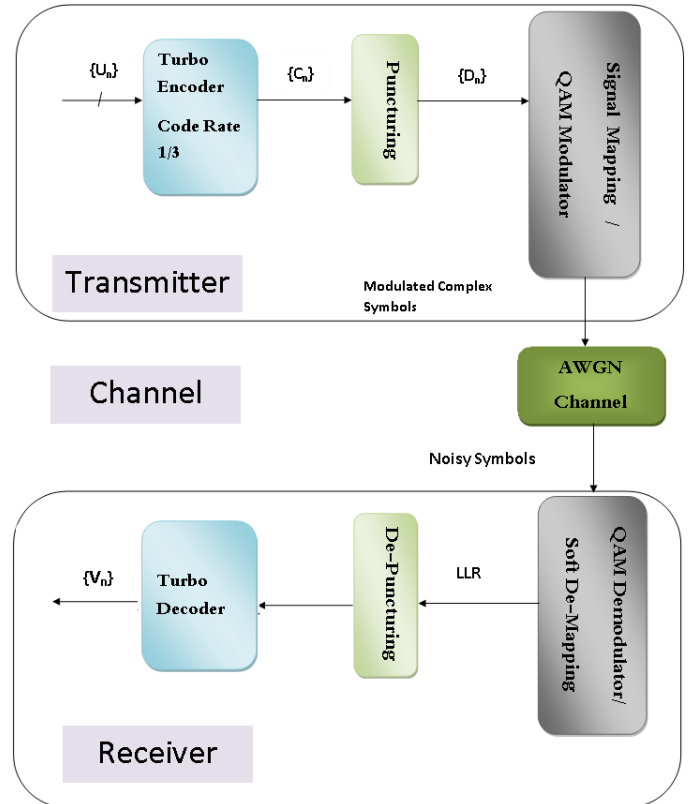

Fig. 1. AMC Proposed System Model

A. Turbo Encoder

The Turbo encoder [5] is composed of two identical Recursive Systematic Convolution (RSC) as it shows in Figure 2. The two coders receive the same input data U_k with reordering via the interleaver. The outputs are composed of three symbols U_k, P_{k1} and P_{k2}. The code rate of the turbo encoder is $CR = \frac{1}{3}$.
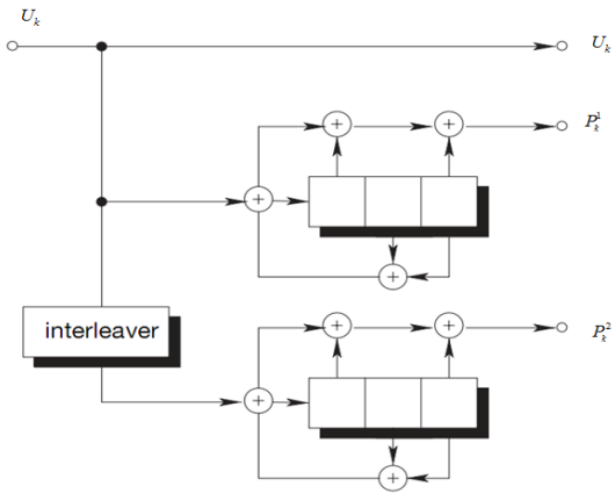
Fig. 2. The Turbo Encoder

B. Puncturing

Puncturing [6] is applied at the outputs of the turbo encoder, to groups of turbo code symbols to reduce the coding rate of the transmitter. The puncturing Matrix contains 1 and 0 to give different code rate $CR = \frac{1}{3}$, $CR = \frac{1}{2}$ and $CR = \frac{2}{3}$ as it shows in Figure 3, Figure 4 and Figure 5.

$$CR = \frac{1}{3}$$

$$P = \begin{pmatrix} 1 & 1 & 1 & 1 & 1 & 1 & 1 & 1 \\ 1 & 1 & 1 & 1 & 1 & 1 & 1 & 1 \\ 1 & 1 & 1 & 1 & 1 & 1 & 1 & 1 \end{pmatrix}$$

Fig. 3. Puncturing matrix with $CR = \frac{1}{3}$

$$CR = \frac{1}{2}$$

$$P = \begin{pmatrix} 1 & 1 & 1 & 1 & 1 & 1 & 1 & 1 \\ 1 & 0 & 1 & 0 & 1 & 0 & 1 & 0 \\ 0 & 1 & 0 & 1 & 0 & 1 & 0 & 1 \end{pmatrix}$$

Fig. 4. Puncturing matrix with $CR = \frac{1}{2}$

$$CR = \frac{2}{3}$$

$$P = \begin{pmatrix} 1 & 1 & 0 & 1 & 1 & 0 & 1 & 1 \\ 0 & 0 & 0 & 0 & 1 & 1 & 1 & 1 \\ 0 & 1 & 1 & 1 & 0 & 1 & 0 & 1 \end{pmatrix}$$

Fig. 5. Puncturing matrix with $CR = \frac{2}{3}$

C. Modulation

In the $M - QAM$ modulation symbols in the inputs are divided into blocks of length $k = log_2(M)$, where M is the rank of the modulation. Each block is connected to one point of the $M - QAM$ modulation [7]. Figure 6, Figure 7 and Figure 8 show respectively the distribution of symbols in

QPSK, $16 - QAM$ and $64 - QAM$ modulations. $QPSK$ with $CR = \frac{1}{2}$ gives 2 bits per symbol, 16-QAM with CR=$\frac{3}{4}$ gives 4 bits per symbol and $64 - QAM$ with $CR = \frac{3}{4}$ gives 6 bits per symbol.
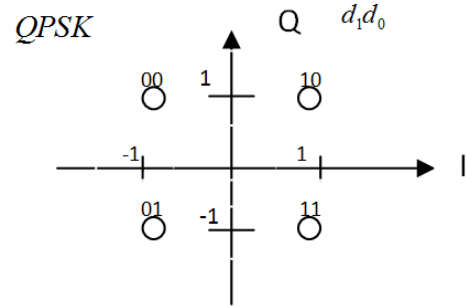

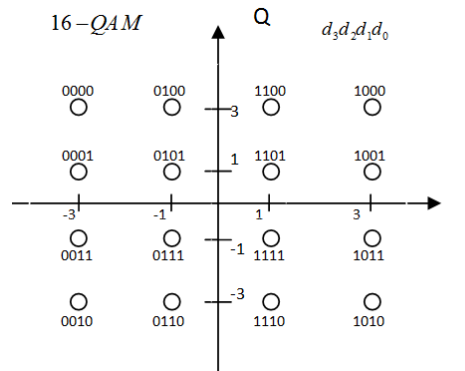Fig. 6. Distribution of symbols in $QPSK$
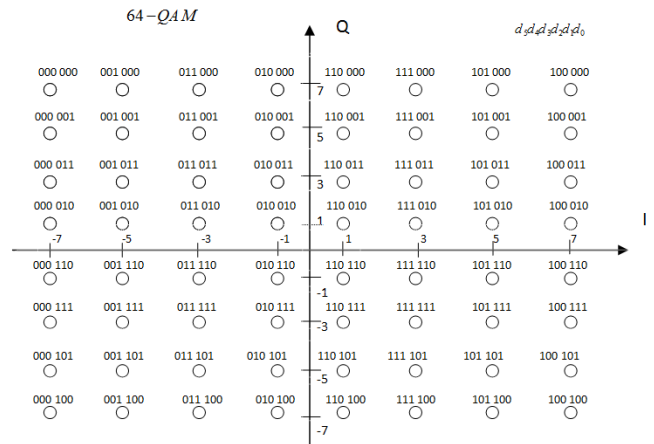

Fig. 7. Distribution of symbols in $16 - QAM$

Fig. 8. Distribution of symbols in $64 - QAM$

D. The Receiver

The channel used is AWGN [8]. At the receiver symbols are demodulated and sent to the decoder which is composed of de-puncturing and Turbo decoder. The de-puncturing uses

the same puncturing matrix to redistribute the symbols in the correct place before the puncturing. The deleted symbols are replaced with zeros. The de-puncturing gives the values to the turbo decoder which concludes the sent symbols [9]. In the following we will explain the results of the simulations.

III. SIMULATION RESULTS OF THE STATIC MODULATION AND CODING

The simulations have been run in MATLAB under AWGN and Rayleigh fading channels [10]. We first present the performance of different types of modulations and coding, then we conclude the table of the threshold of the SNR for the each modulation and coding. Finally we present the throughput in term of SNR in AWGN channel and Rayleigh fading.

A. The Performance of QPSK

Figure 9 depicts the Bite Error Rate (BER) in term of SNR with the scenarios of QPSK modulation without and with code rates of $CR = \frac{1}{3}$, $CR = \frac{1}{2}$, $CR = \frac{2}{3}$. It is shown that the best performance occurs for $CR = \frac{1}{3}$, and the performance decreases with the increase of CR. The figure shows that for a fixed value of $BER = 10^{-4}$, the gain in SNR with coding, comparing to the modulation without coding, is equal to $5dB$, $8dB$ and $12dB$ when $CR = \frac{2}{3}$, $CR = \frac{1}{2}$, $CR = \frac{1}{3}$ respectively.
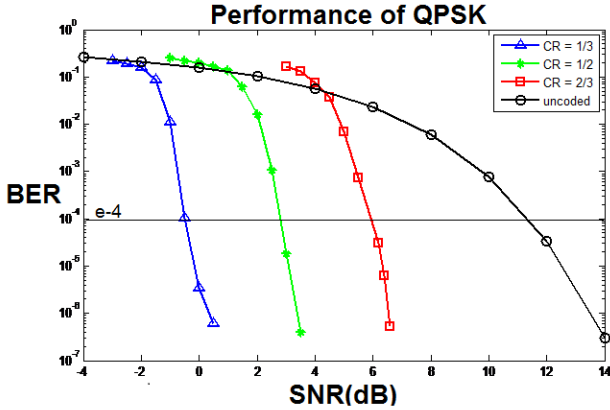

Fig. 9. $QPSK$ Performance

B. The Performance of 16-QAM

Figure 10 depicts the BER in term of SNR with the scenarios of $16 - QAM$ modulation without and with code rates of $CR = \frac{1}{3}$, $CR = \frac{1}{2}$, $CR = \frac{2}{3}$. It is shown that the best performance occurs for $CR = \frac{1}{3}$, and the performance decreases with the increase of CR. The figure shows that for a fixed value of $BER = 10^{-4}$, the gain in SNR with coding, comparing to the modulation without coding, is equal to $5dB$, $9dB$ and $13dB$ when $CR = \frac{2}{3}$, $CR = \frac{1}{2}$, $CR = \frac{1}{3}$ respectively.
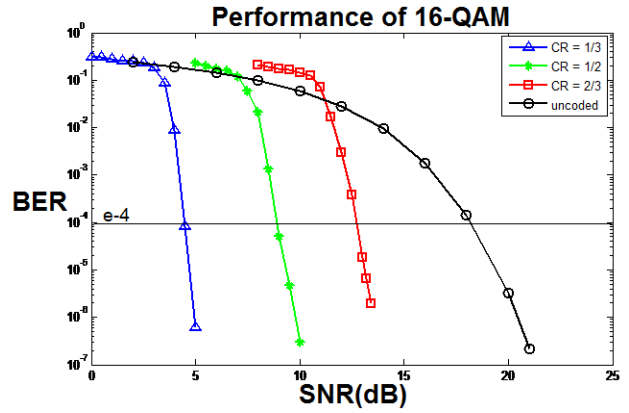

Fig. 10. $16 - QAM$ Performance

C. The Performance of 64-QAM

Figure 11 depicts the BER in term of SNR with the scenarios of $64 - QAM$ modulation without and with code rates of $CR = \frac{1}{3}$, $CR = \frac{1}{2}$, $CR = \frac{2}{3}$. It is shown that the best performance occurs for $CR = \frac{1}{3}$, and the performance decreases with the increase of CR. The figure shows that for a fixed value of $BER = 10^{-4}$, the gain in SNR with coding, comparing to the modulation without coding, is equal to $5dB$, $10dB$ and $15dB$ when $CR = \frac{2}{3}$, $CR = \frac{1}{2}$, $CR = \frac{1}{3}$ respectively.
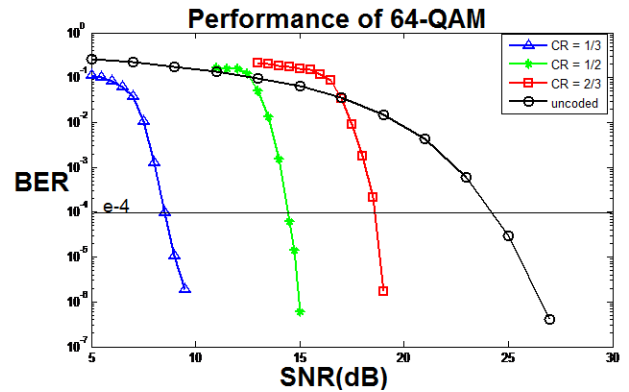

Fig. 11. $64 - QAM$ Performance

D. Comparison of Performances

The figure 12 shows that the performance of $16 - QAM$ with $CR = \frac{1}{3}$ is better than $QPSK$ with $CR = \frac{2}{3}$, though the number of bits per symbol is $\frac{1}{3}$ in both case. The performance of $64 - QAM$ with $CR = \frac{1}{3}$ is better than $16 - QAM$ with $CR = \frac{1}{3}$, though the number of bits per symbol is 2 in both cases.
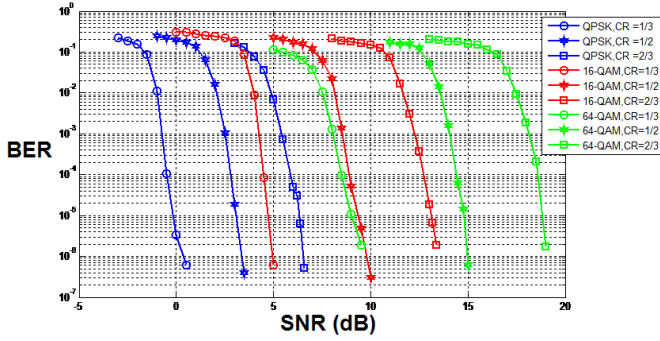
Fig. 12. Performances of different modulation with different code rates

Fig. 15. Throughput in term of SNR in AWGN channel

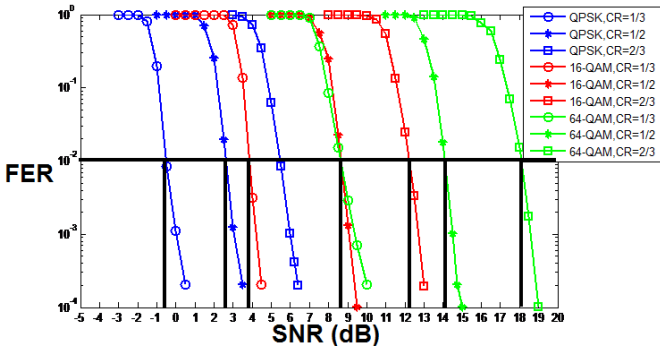Figure 13 shows the Frame Error Rate (FER) in term of SNR for different modulations and coding.

Fig. 13. Frame Error Rate in term of SNR

Figure 14 shows the minimum thresholds of SNR that allows to choose the respective modulation and coding for $FER = 10^{-2}$. We notice that $16 - QAM$ with $CR = \frac{1}{3}$ replaces QPSK with $CR = \frac{2}{3}$, and $64 - QAM$ with $CR = \frac{1}{3}$ replaces $16 - QAM$ with $CR = \frac{1}{2}$.

bpsym	SNR(dB)	CR	Modulation
2/3	–	1/3	$QPSK$
1	3	1/2	$QPSK$
4/3	4	1/3	$16 - QAM$
2	9	1/3	$64 - QAM$
8/3	12.5	2/3	$16 - QAM$
3	14.5	1/2	$64 - QAM$
4	18.5	2/3	$64 - QAM$

Fig. 14. The Minimum threshold for modulation and coding

E. Throughput in term of SNR for AWGN and Rayleigh fading

Figure 15 shows the throughput in the presence of AWGN channel. We notice that $16 - QAM$ with $CR = \frac{1}{3}$ gives higher throughput than $QPSK$ with $CR = \frac{2}{3}$. We also notice that $64 - QAM$ with $CR = \frac{1}{3}$ gives higher throughput than $16 - QAM$ with $CR = \frac{1}{3}$.
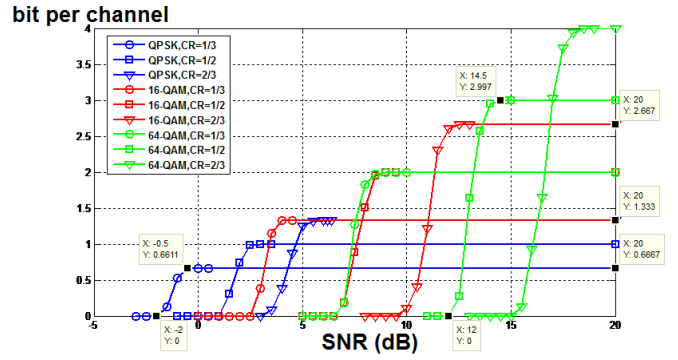
Similar results are obtained in Figure 16 that shows the throughput in the presence of AWGN channel and Rayleigh fading.
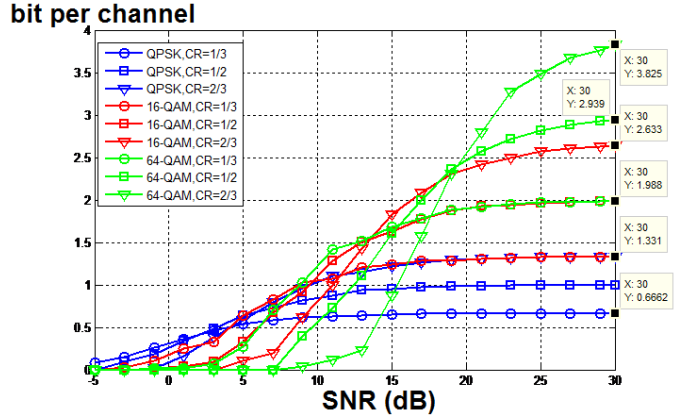

Fig. 16. Throughput in term of SNR in AWGN channel with Rayleigh fading

IV. SIMULATION OF THE ADAPTIVE MODULATION AND CODING

Our simulation of the adaptive modulation and coding is shown in Figure 17. The block diagram is similar to the Figure 1 with the additional Adaptation block. The demodulator at the receiver part calculates the SNR and sends it to the Adaptation block which decides the suitable modulation and coding. Figure 18 shows the curves of the throughput in term of SNR for the adaptive modulation and coding with Rayleigh fading. The curve matches the curve of $QPSK$ and $CR = \frac{1}{3}$ for low values of SNR, and matches the curves of $64 - QAM$ and $CR = \frac{2}{3}$ for high values of SNR. For the medium value of SNR we notice a gain of $4dB$ at $SNR = 15dB$. By consequence the throughput curve of the adaptive modulation and coding acts like an envelope of the maximum values of the throughput of the static modulation and coding.
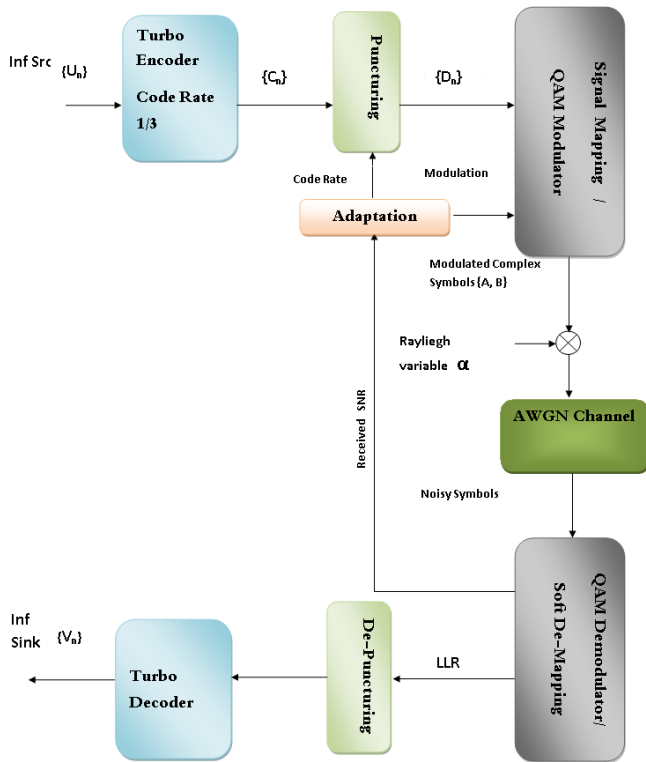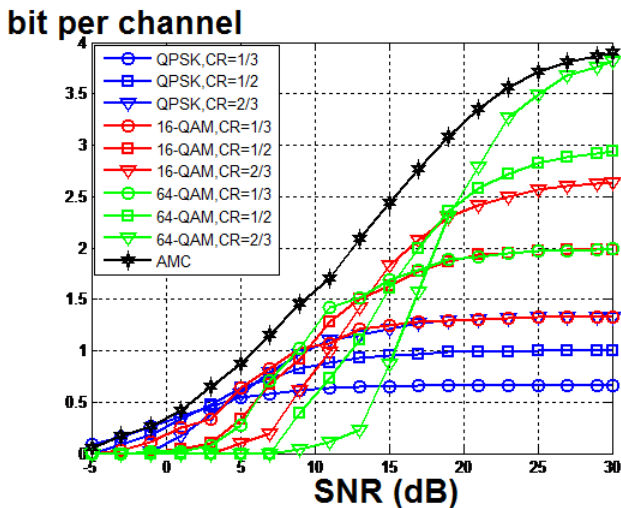
Fig. 17. Throughput of AMC with Rayleigh channel

Fig. 18. Throughput of AMC

V. VALIDATION OF THE AMC SIMULATION RESULTS

To validate our simulation results of the AMC, we use Nemo outdoor and Nemo Analyze tools [11] from one of the mobile operator in the country. The tools allow to measure, store and analyze the parameters of the HSPA+ network between the Node B and the user (e.g. modulation and coding, Energy chip/Noise, Channel Quality Indicator, Number Channelization Code).
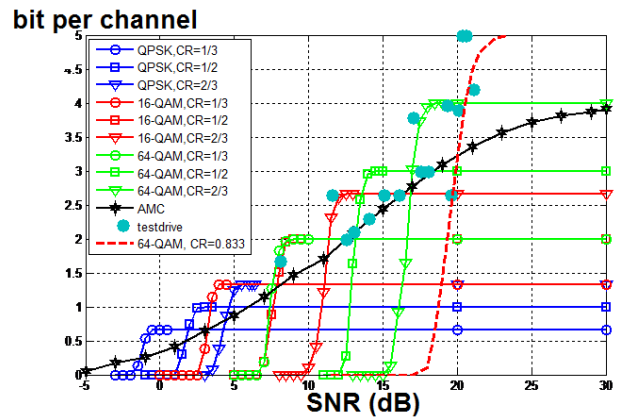

Fig. 19. Throughput of AMC

Figure 19 shows the measured and the simulated throughput in term of SNR for the adaptive modulation and coding. We noticed that most of the points of the measurements are located near the throughput of the adaptive modulation and coding. Some points deviate because of the difference between the real channel and the simulated channel.

VI. CONCLUSION

This paper presented the simulations of the adaptive modulation and coding for mobile communication networks. We concluded that the throughput could be increased by increasing the modulation order and the coding rate with the increase of Signal-to-Noise Ratio. The AMC gives higher throughput by changing the modulation and coding in function of the Signal-to-Noise ration at the receiver with a gain of $4dB$. The simulation results are validated via drive test measurements of HSPA+ mobile network.

REFERENCES

[1] S. Salih and M. Suliman, *Implementation of Adaptive Modulation and Coding Technique using*, International Journal of Scientific and Engineering Research Volume 2, Issue 5, May-2011, ISSN 2229-5518.
[2] S. Kottkamp, *HSPA+ Technology Introduction*, Application Note, Rohde and Schwarz, 2009
[3] S. Hadi and T. Tiong, *Adaptive Modulation and Coding for LTE Wireless Communication*, IOP Conf. Series: Materials Science and Engineering 78, 2015.
[4] M. Fernandez and M. Rupp and M. Wrulich *HSDPA CQI Mapping Optimization Based on Real Network Layouts*, Bachelor Thesis, Institute of Communications and Radio-Frequency Engineering, 2008.
[5] F. Huang T. Pratt, *Evaluation of Soft Output Decoding for Turbo Codes*, Master of Science, Electrical Engineering,ETD etd-71897-15815, 1997.
[6] M. Tuechler and J. Hagenauer. *Channel coding*, lecture script, Munich University of Technology, pp. 111-162, 2003.
[7] J. Proakis, *Digital Communications*, fourth edition, Mc-Graw Hill, 2001
[8] P. Farrell and J. Moreira, *Essentials of Error-Control Coding*, John Wiley and Sons Ltd, 2006.
[9] K. Bogawar, S. Mungale and M. Chavan, *Implementation of Turbo Encoder and Decoder*, International Journal of Engineering Trends and Technology (IJETT), Volume 8 Number 2- Feb 2014.
[10] B. Sklar *Rayleigh Fading Channels in Mobile Digital Communication Systems, Part I: Characterization*,IEEE Communications Magazine, July 1997.
[11] T. Nugraha *Drive Test Nemo*,Technology, Business, Aug 19, 2012.